Solar-Terrestrial Physics. 2026, vol. 12, iss. 1, pp. 87–97. DOI: 10.12737/stp-121202610. © 2026 O.M. Lebed, S.V. Pilgaev, A.V. Larchenko, N.F. Blagoveshchenskaya, A.S. Kalishin, T.D. Borisova, O.Yu. Stribny, M.V. Filatov, M.V. Kuznetsova, A.S. Nikitenko, E.B. Beketova, Yu.V. Fedorenko. Published by INFRA-M Academic Publishing House

DOI: 10.12737/stp-121202610
EDN: NWTOOS

Received June 09, 2025
Accepted November 11, 2025

THE FIRST RESULTS OF OBSERVATIONS OF AURORAL HISS DURING THE "NORTH POLE–41" EXPEDITION

O.M. Lebed
Polar Geophysical Institute, Apatity, Russia, olga.m.lebed@gmail.com

S.V. Pilgaev
Polar Geophysical Institute, Apatity, Russia, pilgaev@pgia.ru

A.V. Larchenko
Polar Geophysical Institute, Apatity, Russia, alexey.larchenko@gmail.com

N.F. Blagoveshchenskaya
Arctic and Antarctic Research Institute, Saint Petersburg, Russia, nataly@aari.nw.ru

A.S. Kalishin
Arctic and Antarctic Research Institute, Saint Petersburg, Russia, askalishin@aari.ru

T.D. Borisova
Arctic and Antarctic Research Institute, Saint Petersburg, Russia, borisova@aari.ru

O.Yu. Stribny
Arctic and Antarctic Research Institute, Saint Petersburg, Russia, rd1a@mail.ru

M.V. Filatov
Polar Geophysical Institute, Apatity, Russia, mijgun@yandex.ru

M.V. Kuznetsova
Polar Geophysical Institute, Apatity, Russia, kuznetsova@pgia.ru

A.S. Nikitenko
Polar Geophysical Institute, Apatity, Russia, alex.nikitenko91@gmail.com

E.B. Beketova
Apatity Branch of Murmansk Arctic University, Apatity, Russia, elena.beketova@gmail.com

Yu.V. Fedorenko
Polar Geophysical Institute, Apatity, Russia, yury.fedorenko@gmail.com

Abstract. During the North Pole–41 expedition, three components of the VLF electromagnetic field were simultaneously measured on a drifting ice-resistant platform and at the Lovozero and Barentsburg observatories. We consider three VLF events that occurred in magnetically quiet time. During two of them (the events on January 24, 2023 and March 12, 2024), auroral hiss bursts were recorded at three stations located in the auroral and circumpolar regions and spaced up to 2.600 km apart. The spectral and temporal characteristics of the bursts at all the stations were almost the same. The fact that hiss was recorded with the same properties at such large distances can be explained under the assumption of a homogeneous flow of auroral electrons with energies from 0.1 to 10 keV throughout the precipitation area, which generate quasi-electrostatic waves at altitudes 10–20 thousand km, along with the simultaneous presence of small-scale ionospheric irregularities in the vicinity of all three stations, where these waves are scattered into the propagation cone to the Earth surface. We examine the case of hiss recording (the January 25, 2023 event) demonstrating the locality of the hiss recording area during one day — a hiss burst is first observed at one station, then at another. This is probably due to the appearance/disappearance of local areas of small-scale irregularities, where quasi-electrostatic waves are scattered providing propagation to the Earth surface.

Keywords: auroral hiss, ionosphere, VLF wave.

INTRODUCTION

Low-frequency electromagnetic emissions are one of the sources of information about near-Earth plasma conditions. Nowadays, despite the widespread use of satellite data, the application of ground-based detection results to the analysis of VLF events remains an urgent challenge, especially at high latitudes, where precipitation of charged particles can lead to rapid changes in ionospheric conditions. Ground-based observations make it possible to separate temporal variations of the field from spatial ones, caused by satellite motion, and to study the dynamics of long-lasting processes that determine the space-time structure of the radiation field near the Earth surface. Investigations into geophysical processes based on ground-based observations of VLF electromagnetic fields in circumpolar latitudes of the Arctic are of great interest in understanding physical processes in the dayside polar cusp and the polar cap, where there is direct access of solar wind plasma to the ionosphere. This is necessary both to improve space weather prediction and to examine the effect of heliogeophysical disturbances on ionospheric conditions and hence on the quality of short-wave communication. Due to the lack of continuously operating observatories, measurements of VLF electromagnetic

fields at circumpolar latitudes of the Arctic are performed during marine expeditions or at drifting stations.

During the marine expedition Transarctica–2019, organized by the Arctic and Antarctic Research Institute (AARI) from March 20 to May 20, 2019, the scientific expedition vessel Akademik Treshnikov was frozen in ice north of the Franz Josef Archipelago from which it began to drift. One of the objectives of the expedition was to study the space-time structure of VLF emissions of magnetospheric origin observed on the Earth surface. For this purpose, a multifunctional digital VLF receiver was employed which provided digital recording of two horizontal magnetic and vertical electric components of the field, being precisely synchronized with Universal Time [Pilgaev et al., 2021]. During this expedition, several VLF events were recorded, mainly auroral hiss bursts [Pilgaev et al., 2020].

In 2022–2024, AARI specialists organized the North Pole–41 (NP–41) expedition at the drifting polar station. Low-frequency observations were carried out by a VLF receiver identical to that exploited in the Transarctica-2019 expedition. The same stationary receivers were used for observations at the Barentsburg Observatory (78.09° N, 14.21° E), also located in the circumpolar region, but west of the drift trajectory, and at the Lovozero Observatory (67.98° N, 35.082° E), situated in the auroral zone. Throughout the observation period in this expedition from December 1, 2022 to March 30, 2024, VLF emissions of magnetospheric origin were generally auroral hisses.

Auroral hisses are one of the most frequently recorded types of natural low-frequency emission at high latitudes [Makita, 1979; Sazhin et al., 1993]. In Russian-language literature, they are often referred to as auroral hiss [Kleimenova et al., 2019]. Auroral hiss is an electromagnetic noise emission detected in the VLF band (very low frequency, 3–30 kHz) with a maximum intensity at 8–10 kHz frequencies. It is generally thought that auroral hiss is generated in the form of quasi-electrostatic waves in the magnetosphere at altitudes ~5–20 thousand km and is associated with precipitation of soft electrons (with energies from 0.1 to 10 keV) [Sonwalkar, Harikumar, 2000; Makita, 1979]. Low–orbit satellites record auroral hiss at almost every crossing of auroral latitudes in the evening and at night, with a maximum intensity at ~68°N – 72° N [Gurnett, 1966]. However, of 140 cases of hisses observed by a satellite, only two were accompanied by the simultaneous occurrence of hiss on Earth. Many authors state that auroral hiss usually correlates closely with local geomagnetic activity, but this statement is controversial. In particular, Jørgensen and Ungstrup [1962] did not find such a correlation in VLF data on Greenland, but Harang and Larsen [1965] showed a positive correlation between the occurrence of hiss in auroral latitudes and local moderate geomagnetic disturbances and a negative correlation in the case of strong disturbances. Manninen et al. [2020], using auroral hiss data from the Finnish station Kannuslehto (geomagnetic latitude 64.2° N) for 2015–2018, have revealed that the occurrence of auroral VLF emissions in the equatorial region of the auroral oval is a typical feature of the development phase of a substorm. During this period, 98 isolated and rather powerful magnetic substorms were recorded over Scandinavia. In 93 % of the substorms considered, auroral hiss was observed simultaneously with an increase in field-aligned currents. Field-aligned currents are caused by precipitation of soft electrons, which are a likely source of auroral hiss.

Due to the fact that the modulus of the horizontal component of the refractive index vector of quasi—electrostatic waves is much larger than 1, penetration of auroral hiss into the Earth–ionosphere waveguide and its recording on the Earth surface are possible only after scattering by small-scale (comparable with the quasi-electrostatic wave length) electron density irregularities of the upper ionosphere [Sonwalkar, Harikumar, 2000]. In this case, scattering has to occur before quasi-electrostatic waves reach a height, where the frequency of the lower hybrid resonance (LHR) ω_{LHR} becomes equal to the wave frequency,

$$\omega_{LHR}^2 = \frac{1}{M_{eff}} \frac{\omega_{Pe}^2 \omega_{He}^2}{\omega_{Pe}^2 + \omega_{He}^2}, \quad \frac{1}{M_{eff}} = \frac{m_e}{n_e} \sum_i \frac{n_i}{m_i}.$$

Here, ω_{Pe}, ω_{He} are the plasma frequency and the electron gyrofrequency; m_e, n_e are the electron mass and density; m_i, n_i are the mass and concentration of the ith ion component [Budden, 1985; Kimura, 1966; Stix, 1992]. For 8–10 kHz frequencies, this height lies in the range 800–1200 km. The calculations made in [Nikitenko et al., 2023] have shown that the frequently observed locality of the area illuminated by auroral hiss on the Earth surface can only be explained if the region of irregularities is located at an altitude that is close to and slightly higher than that of LHR.

The size of the illuminated area on the Earth surface is mainly determined by the size of the region of irregularities in the upper ionosphere and the size of the cross-section of a packet of quasi-electrostatic waves incident on this region [Nikitenko et al., 2023]. The Cherenkov resonance condition [Sazhin et al., 1993], which relates the longitudinal component of the wave normal of a generated quasi-electrostatic wave to the longitudinal velocity of an electron, does not define the direction of the component perpendicular to the geomagnetic field line. In ray tracing modeling of quasi-electrostatic wave propagation from 10–20 thousand km to the height of irregularities, the distribution of directions of this component was assumed to be uniform in the range $[-\pi, \pi)$ [Nikitenko et al., 2023]. The modeling results indicate that the meridional plane cross-section of the illuminated area of irregularities has two zones 300–400 km wide, one of which is located closer to the equator, and the other is closer to the pole symmetrically at the footprint of a magnetic field line on which generation occurs, and quasi-electrostatic waves do not enter the area near this field line.

To estimate the minimum size of the illuminated area on the Earth surface, Nikitenko et al. [2023] have modeled the amplitude distribution of the magnetic field horizontal component when quasi-electrostatic waves are scattered from a 50 km region located at an altitude of 800 km. It has been found that 90 % of the radiation

power falls into a circle ~400 km in diameter, and the area, in which the root mean square (RMS) signal amplitude is at least –20 dB from the maximum, is ~150–200 km.

Yearby and Smith [1994] proposed to use the polarization index B_t for estimating the distance from the VLF wave ionospheric exit point to the observation point. The algorithms described in that paper may be good for whistlers, but they are unlikely to be suitable for VLF hisses due to the random nature of their field. More correct analysis of the relationship of polarization of hiss observed on the Earth surface with distance has been carried out in [Nikitenko et al., 2021]. It follows from Figure 2 of that work that the polarization of the horizontal magnetic field on the Earth surface near the center of the scattering region in the Northern Hemisphere is always right-hand and remains so at a distance 100–150 km. At a distance ~350–400 km from the center, it changes to left-hand. These distances weakly depend on the electron density profile of the lower ionosphere and can be specified for each individual event by modeling.

Observations of natural VLF emissions in circumpolar regions are episodic, so the measurement results obtained during the NP-41 expedition are important for understanding VLF wave generation and propagation in the polar cap. This paper discusses the most interesting results of observations of auroral hiss bursts recorded at the drifting polar station in neutral waters. The observational results are compared with observations of VLF emissions at the Barentsburg (BAB) and Lovozero (LOZ) observatories.

EXPERIMENT

The North Pole–41 expedition, organized by AARI, was undertaken from October 2, 2022 to May 7, 2024 on a drifting ice-resistant platform (LSP), which drifted under the influence of currents and wind in the Arctic Basin of the Arctic Ocean. The special feature of this expedition was that the platform was the research vessel North Pole frozen in ice and drifting with it. The platform made measurements in various fields of science, in particular in meteorology, geophysics, hydroacoustics, oceanography, etc. In addition, antenna masts of a multifunctional digital VLF receiver were installed on the ice 500 m from the vessel, which provided recording of two horizontal magnetic (B_x, B_y) and vertical electric (E_z) field components, being precisely synchronized with Universal Time (Figure 1, *a*).

The VLF receiver was used to make continuous observations of the electromagnetic field components in a wide frequency range (from 300 Hz to 15 kHz) [Pilgaev et al., 2021]. Its characteristic features are galvanic isolation of digital and analog parts, which minimizes the level of industrial noise in the E_z component, and precise synchronization of each received digital data sample with Universal Time with a maximum error not exceeding 1 ms. Recording the three field components allows us to determine not only the standard set of parameters of the measured electromagnetic field (amplitudes and parameters of the polarization ellipse), but also the magnitude and direction of the Poynting vector, which significantly increases the information content of observations. Measuring channels of each of the VLF receivers employed were calibrated using the device and method described in [Pilgaev et al., 2018].

Figure 1, *b* presents a map of the LSP drift path (black line), as well as coordinates of the Barentsburg and Lovozero observatories (the distance between them is 1300 km). At the beginning of 2023, the platform was in the circumpolar region, while by the beginning of 2024 it had shifted closer to the Spitsbergen archipelago. If we look at the position of the platform in geomagnetic coordinates (geomagnetic parallels are indicated by red lines in Figure 1; and geomagnetic latitudes, by numbers), it turns out that LSP was located between 75° N and 79° N (near the polar cap) during the experiment.

While the VLF receiver antennas were at a sufficient distance away from the main source of noise (the research vessel), about a quarter of all recordings were corrupted by noise of unknown origin, which necessitates a closer look at the electromagnetic compatibility of the geophysical instruments used in the NP–41 expedition. A number of observations were also periodically interrupted due to different reasons, including shearing of ice. In total, for ~1.5 years of ice platform drift, ~8 months of recordings of VLF electromagnetic field components were obtained.

DATA PROCESSING

Auroral hiss recorded near the Earth surface can be considered as a quasi-stationary Gaussian three-dimensional random process with zero mean and a slowly time-varying covariance matrix **J** [Means, 1972; Rytov, 1966]. To calculate the matrix, the sequences of readings of the electromagnetic field components $B_x(t)$, $B_y(t)$, and $E_z(t)$ in the selected interval $[0, t_{max}]$ are broken up into N fragments. The duration of each fragment Δt is selected according to the time rate of change in the covariance matrix elements. Elements of the kth fragment, k=1.... N, are calculated as the product of Fourier transforms of the components in this fragment $B_x(\omega)$, $B_y(\omega)$, and $E_z(\omega)$.

$$\mathbf{J_k} = \begin{bmatrix} E_z(\omega)E_z^*(\omega) & E_z(\omega)B_x^*(\omega) & E_z(\omega)B_y^*(\omega) \\ B_x(\omega)E_z^*(\omega) & B_x(\omega)B_x^*(\omega) & B_x(\omega)B_y^*(\omega) \\ B_y(\omega)E_z^*(\omega) & B_y(\omega)B_x^*(\omega) & B_y(\omega)B_y^*(\omega) \end{bmatrix} = \begin{bmatrix} J_{11} & J_{12} & J_{13} \\ J_{12}^* & J_{22} & J_{23} \\ J_{13}^* & J_{23}^* & J_{33} \end{bmatrix}.$$

The asterisk here marks a complex conjugation.

The LSP initial data on electromagnetic field components needed to be preprocessed since they contained all kinds of noise, both impulse and quasi-stationary. Impulse noise includes noise from long-distance lightning discharges — atmospherics. The average spectral power density of atmospherics is especially high in the frequency range from 3–4 kHz to tens of kilohertz, which coincides with the frequencies of the maximum

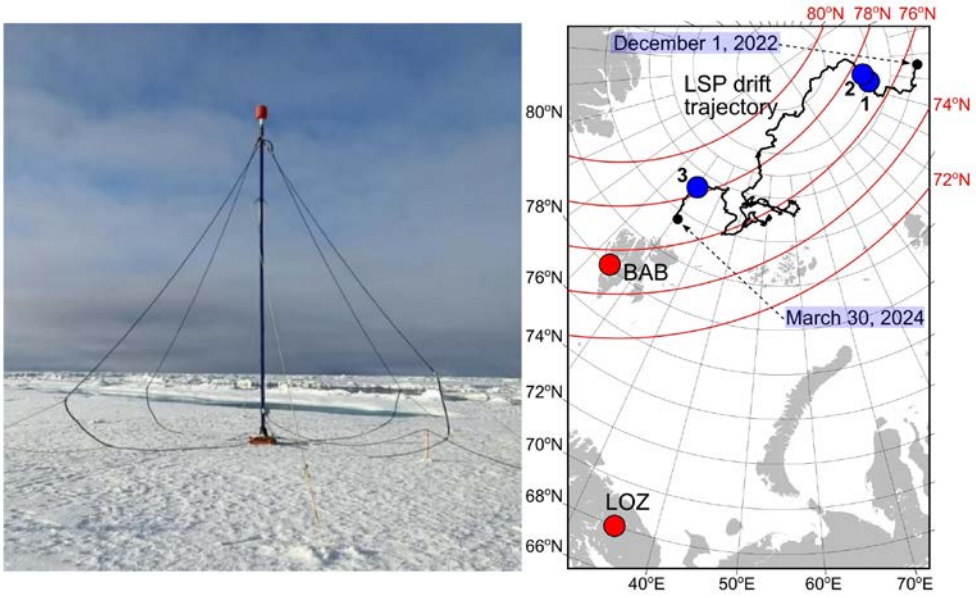

Figure 1. A photo from the installation site of VLF receiver antennas (*a*) and a map (*b*) indicating the locations of the Barentsburg (BAB, Spitsbergen archipelago), Lovozero (LOZ, Kola Peninsula) observatories, and LSP drift (black line). Red lines are geomagnetic parallels. Numbers represent the location of LSP during the events of interest: 1 — January 24, 2023, 12:00 UT; 2 — January 25, 2023, 04:00 and 12:00 UT; 3 — March 12, 2024, 16:00 UT

intensity of auroral hiss (8–10 kHz) and can exceed its spectral power density by several orders of magnitude. Quasi-stationary noise comprises 50 Hz harmonics from power transmission lines, 82 Hz harmonics that occur when a powerful low-frequency transmitter is switched on for communication with submarines, and other quasi-harmonic noises. Short impulse noise with a wide frequency spectrum can be eliminated only in the time domain, whereas quasi-stationary noise that varies slowly over time is suppressed in the frequency domain. Signal processing methods have been tested and are currently being used to process low-frequency emission recordings at the Lovozero and Barentsburg observatories [Lebed et al., 2019].The method of suppressing impulses of atmospherics, widely used by researchers from the Finnish Observatory Sodankylä to analyze VLF observations at the Kannuslehto station [Manninen et al., 2013], boils down to isolating impulses in a signal and excluding them from further processing. The atmospheric detector is triggered when the envelope of the magnetic field exceeds a certain threshold whose value is selected by trial and error and does not change further. The most important difference in the atmospheric suppressor employed in this work is the use of an adaptive threshold for detector operation and a time window whose duration depends on the atmospheric impulse duration. Note that it is impossible to completely remove atmospherics from recordings of the field components since the signal and the atmospherics superimposed on it cannot be separated.

Quasi-stationary noise was eliminated in the frequency range 200–3000 Hz, where its spectral power density significantly exceeded the noise level. When removing 50 Hz harmonics, the current frequency of its third harmonic was first searched for. Then the frequencies of higher-order harmonics were calculated. These harmonics were cut out using narrowband filtering by a bandpass filter with a bandwidth varying from 3 to 10 Hz when harmonic frequencies changed from 500 Hz to 5 kHz. Suppose that the elements of the covariance matrix **J** slowly change in frequency. In this case, the gaps formed after cutting out the harmonics are filled with complex white delta-time-correlated Gaussian noise with a covariance matrix corresponding to the average matrix calculated from the spectra at edges of the removed frequency band. This algorithm has also been employed to remove 82 Hz noise, harmonics and is suitable for suppressing any narrowband noise signals with fixed or slowly varying frequencies.

In this paper, using the **J** elements, we estimate the auroral hiss field parameters such as the power spectral density of the magnetic field horizontal component $B_t^2 = J_{22} + J_{33}$, the RMS value of the magnetic field horizontal component $RMS_B = \left(B_t^2 \Delta f\right)^{1/2}$, where Δf is the frequency band in which it is calculated, and the azimuth angle of the Poynting vector $\varphi_p = \text{atan2}\left(-\text{Re}\left(J_{12}\right), \text{Re}\left(J_{13}\right)\right)$. Unlike the usual function arctan(y/x), which returns the result in the range [–π/2, π/2], the function atan2(y, x) uses the signs of arguments to determine the quadrant in which the vector lies, and returns the result over the entire angular range [–π, π]. To analyze the magnetic field polarization, it is convenient to employ the circular polarization index $P_c = 2\text{Im}\left(J_{23}\right)/\left(J_{22} + J_{33}\right)$ [Rytov, 1966], which is also expressed in terms of the covariance matrix elements. The circular polarization index varies between [–1, +1], is positive for right-hand circularly polarized waves, and negative for left-hand circularly polarized waves. The proximity of P_c to zero indicates linear polarization.

It is worth noting that the results of analysis of auroral hiss arrival angles depend not only on the accuracy of measurements of field components, but also on the accuracy of determining the orientation of measuring antennas. A peculiarity of the NP–41 expedition was the continuous drift of the ice platform resulting in that the position of the research vessel along with the VLF receiver antennas constantly changed. Despite the fact that the vessel's azimuth was recorded throughout the experiment, in 2024, due to shearing of ice, the receiver antennas were transferred and it became necessary to verify their direction. For this purpose, we applied signals from transmitters of the RSDN-20 (Alpha) radionavigation system, which emit at VLF frequencies of 11.9, 12.6, and 14.9 kHz. These transmitters are located in Revda, Novosibirsk, Krasnodar, and Komsomolsk-on-Amur. Numerous studies of propagation characteristics of signals from the VLF transmitters in the Earth–ionosphere waveguide have shown that at distances of more than 1000 km a radio signal propagates along the great circle arc connecting a transmitter and a receiver, which was used for the verification. The propagation direction was calculated from the covariance matrix components. Comparison of the calculated signal propagation direction with the expected direction to the transmitter allows us to take into account the current orientation of the antennas while processing.

Additional information about the random nature of auroral hiss recorded on the Earth surface can be obtained by estimating the probability density function of its field parameters. Since the direction of wave arrival at the observation point is of interest, to account for the random structure of the field we calculated energy flux density distribution over the azimuth angle of the vector oppositely directed to the Poynting vector — backazimuth $\varphi_{bp}=_p+180°$. To do this, we selected a segment of field component records with lengths so long as to ensure the statistical stability of the estimate and so short as to provide acceptable time resolution. For the selected segment, its spectrum was plotted and a frequency band was chosen to calculate the estimate. For each reading belonging to the segment, we computed the backazimuth $\varphi_{bp}(k)$ and the power flux density, represented by a vector whose direction is opposite to the direction of the Poynting vector.

$$S(k)=\left[\left(\mathrm{Re}(J_{12})\right)^2+\left(\mathrm{Re}(J_{13})\right)^2\right]^{1/2},$$

where k is the number of reading; k=1, 2, ... K, K is the number of readings in the segment. The range of possible backazimuth values (0.2π) was divided into N intervals of equal width. Then, a sample S_1, S_2, ..., S_N was formed from the K set, including S readings with backazimuth values falling within the angular range i=1, 2, ... N. The estimate of the energy flux density distribution over the backazimuth was calculated as the sum of elements of each S_i set divided by K and by the cell width. In this case, the maximum of the S distribution by the backazimuth φ_{bp} indicates the most likely direction to the region of hiss exit from the ionosphere to the Earth surface, opposite to the direction of the energy flux vector at the observation point.

OBSERVATIONAL RESULTS AND DISCUSSION

In this section, we examine some of the most interesting cases of auroral hiss bursts recorded on the ice–resistant platform during the NP-41 experiment and compare the observational results obtained at the Lovozero and Barentsburg observatories.

The January 24, 2023 event

The first event in question, which occurred on January 24, 2023 at 12:00 UT, demonstrates recording of auroral hiss at the three stations at a time. LSP was then located at 85.8° N, 137.6° E, the distance between the platform and the Lovozero Observatory was 2600 km; and between the platform and the Barentsburg Observatory, 1630 km. At that time, the index AL=–20 nT, Dst=–9 nT, which characterizes quiet geomagnetic conditions.

Figure 2, *a* displays spectrograms of the power spectral density of the horizontal magnetic field component at the three stations. Vertical dark stripes in the spectrogram, constructed from LSP data, are data gaps in the source file. Hiss bursts in the spectrograms are seen to practically coincide at all the stations. To take a closer look at the hiss behavior over time, Figure 3 *a* depicts RMS_B — envelopes B_t calculated in the frequency band 8–9 kHz, where auroral hiss has a maximum intensity, from 12:30 to 12:46 UT. It is obvious that two short bursts of the entire set stand out which were significant in amplitude and actually occurred at the three stations at the same time — those recorded at the 36th and 39th minutes.

Note that the amplitude of these hiss bursts on LSP was ~1.5 times higher than at BAB, and ~2.5 times higher than at LOZ. Figure 2, *c* exhibits the circular polarization index. At LOZ and BAB, it takes values near zero, which indicates linear polarization of waves. According to LSP data, the P_c index is –0.26 and –0.37 for the first and second hiss bursts respectively. The weak left-hand polarization here may suggest that LSP was 300–400 km away from the hiss exit region.

The hiss bursts considered occurred simultaneously at the three stations. Envelopes of these bursts are similar in shape and differ in small details. To explain the similarity between the bursts at large distances, we can assume that the scattering was performed in an isolated local region of ionospheric irregularities. Scattered waves with wave normals trapped in the propagation cone to the Earth surface entered the Earth—ionosphere waveguide and subsequently, propagating in it with low attenuation, caused the simultaneous occurrence of similar-shaped bursts at distances of several thousand kilometers. In this case, the spatial distribution of properties of the auroral electron flux that triggered the generation of auroral hiss bursts is of no importance. This assumption, however, contradicts both the simulation results [Nikitenko et al., 2021] and the experimental observations of auroral hiss at the stations located at distances of several hundred kilometers. The auroral hiss bursts recorded at the Kannuslehto— Lovozero stations do not very often reveal such a similarity between envelope shapes as was recorded in the case

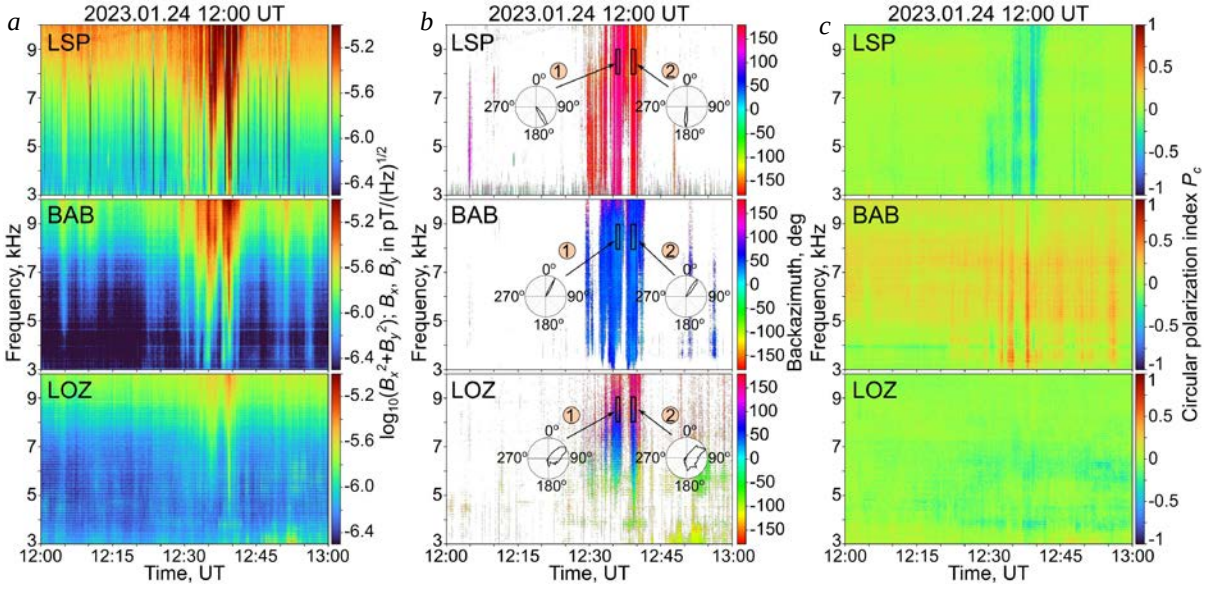

Figure 2. Time and frequency dependences of the spectral power density B_t (*a*), time-averaged φ_{bp} (*b*) and P_c (*c*) on LSP, at the Barentsburg and Lovozero observatories (from top to bottom) for 12:00–13:00 UT on January 24, 2023. Additionally, the central panel illustrates normalized distributions of the energy flux density by φ_{bp} in polar coordinates for the selected sections of the spectrograms

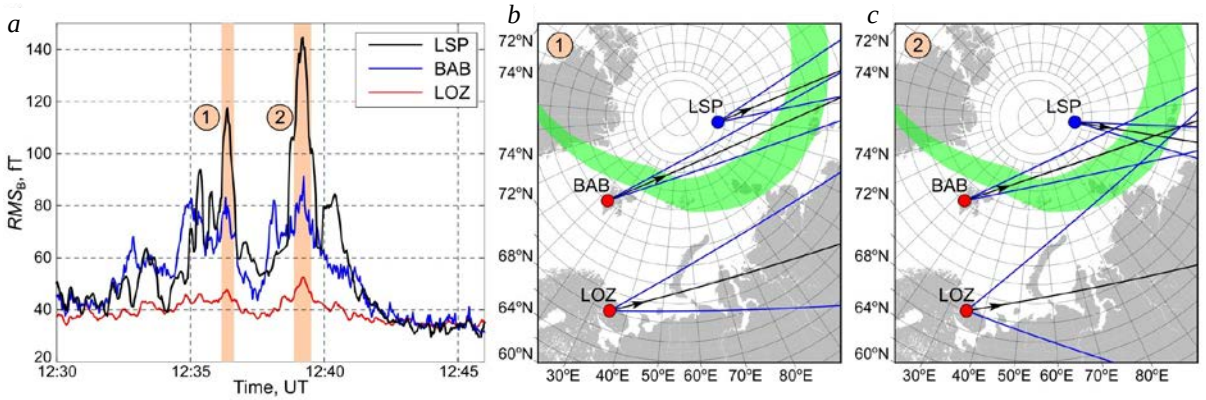

Figure 3. Time dependences of RMS_B in the 8–9 kHz frequency band for three stations: LSP (black curve), BAB (blue curve), and LOZ (red curve) for January 24, 2023 (*a*); maps of the most likely direction to the hiss exit region (black line with arrow), and the range of possible directions (area bounded by blue lines) for the first and second bursts respectively (*b*, *c*). The green color highlights the auroral oval region according to the model [http://apm.pgia.ru/]

of interest at the distance of several thousand kilometers. It follows that the assumption of auroral hiss propagation in the Earth—ionosphere waveguide over such long distances is improbable.

The absence of geomagnetic disturbances is characteristic of the January 24, 2023 event under study. It is fair to assume that under these conditions properties of the flux of soft precipitating electrons, which can induce the generation of quasi-electrostatic waves, differ little along the entire precipitation region. In this case, at altitudes of ~10 to 20 thousand km along the entire precipitation region, packets of random quasi-electrostatic waves, whose average power values will coincide, will propagate to Earth. If there are small-scale ionospheric irregularities, which provide scattering of quasi-electrostatic waves into the cone of propagation to the Earth surface, at distances up to 300–400 km from each station at heights slightly larger than that of LHR, envelopes of auroral hiss bursts similar in shape will be observed at the stations.

In Figure 2, *b* are spectrograms of time-averaged values of the azimuth angle φ_{bp} of the vector oppositely directed to the Poynting vector for the three stations. When constructing the spectrograms, only those φ_{bp} values were used for which the corresponding B_t exceeded the 0.85th quantile, i.e. they were higher than 85 % of all B_t values. The remaining values were highlighted in white. This was done to cut off the noise component of signals. It follows from Figure 2 that at all three stations the φ_{bp} angle remained virtually unchanged from burst to burst. The frequency dependence of the φ_{bp} angle obtained at LOZ is likely due to the fact that the signal power at this station is quite low and there is a high proportion of atmospheric noise in it, which we failed to completely suppress during data preprocessing.

In order to thoroughly examine the behavior of φ_{bp} angles for the simultaneous bursts at the three stations, we have plotted energy flux density distribution over backazimuth angles in the 8–9 kHz frequency range. The regions in question are marked in the central panel of Figure 2 with rectangles, the said distributions are in polar coordinates and shown nearby. Figure 3, *b*, *c* presents ranges of possible directions for the hiss exit region, which were derived from the distributions. Also mapped is the auroral oval precipitation region obtained by the model [Vorobjev, Yagodkina, 2007] for a given moment in time and corresponding geomagnetic conditions [http://apm.pgia.ru/]. The auroral hiss bursts of similar shape are seen to come to LSP and BAB from different areas of the precipitation region, which supports the assumption that an electron flux is uniform in space. The wide range of energy flux density directions at the Lovozero Observatory may be due to the close scattering region, but this is contradicted by the linear polarization of the magnetic field. The spread of directions is most likely related to the influence of noise.

The January 25, 2023 event

Auroral hiss on January 25, 2023 at 04:12 UT was recorded only on LSP, and 8 hrs later, at 12:52 UT, only at BAB. This case when bursts are observed only at one of the stations suggests that the hiss exit region is local. At that time, the platform was drifting near a point with coordinates 85.9° N, 138.7° E. The distance between the platform and LOZ was 2600 km; and the distance between the platform and BAB, 1630 km. Geomagnetic conditions were quiet: *AL*=–10 nT, *Dst*=–12 nT.

Figure 4, *a* presents spectrograms of the spectral density B_t of the above-mentioned auroral hiss bursts on LSP and at BAB. Figure 5, *a*, *c* illustrates envelopes B_t in the 8–9 kHz frequency band at all stations from 04:00 to 04:25 UT and from 12:38 to 13:00 UT respectively. In both cases, the hiss is seen to be only at one of the stations, and envelope amplitudes of its bursts are comparable to the amplitudes of the January 24, 2023 event. Figure 4, *c* shows P_c spectrograms. Both auroral hiss bursts are seen to have a right-hand circular polarization: $P_{c_{LSP}} = 0.8$, $P_{c_{BAB}} = 0.44$, which is typical of a close exit region. Figure 4, *b* offers spectrograms of azimuth angles φ_{bp} for 04:00–05:00 UT and 12:00–13:00 UT on January 25, 2023 according to LSP and BAB data. Also shown are distributions of the energy flux density by φ_{bp} of the most powerful bursts. As in the first case, we mapped the ranges of possible directions for the hiss exit region, as well as the auroral oval (see Figure 5, *b*, *d*).

While BAB at 04:12 UT was located in the precipitation region predicted by the model [Vorobjev, Yagodkina, 2007], hiss was not recorded there. The conditions for generating quasi-electrostatic waves must not have been realized at BAB. The hiss burst at 04:12 UT was recorded only on LSP located in the immediate vicinity of the auroral oval, with the burst energy flux coming from the direction opposite to the location of the precipitation region. This can be explained by using the results from [Nikitenko et al., 2023], where it is shown that the meridional plane cross-section of the illuminated area of irregularities has two zones 300–400 km wide, one of which is located closer to the equator, and the other is closer to the pole symmetrically relative to the footprint of the magnetic field line on which the generation occurs. It can be assumed that the burst waves come from a zone located closer to the pole than the station itself.

At 12:52 UT, the individual hiss burst was recorded only at BAB. All measured parameters of the burst conform to the popular notion of scattering of a quasi-electrostatic wave packet on the local region of irregularities located near BAB. The direction to the region from which waves arrive at the recording point coincides with the expected direction to the precipitation region. The positive polarization index P_c=0.44 suggests that the region of wave propagation to the Earth surface is close to the recording point. It follows that the wave scattering region and BAB are located close to each other and near the precipitation region, as shown in Figure 5, *d*.

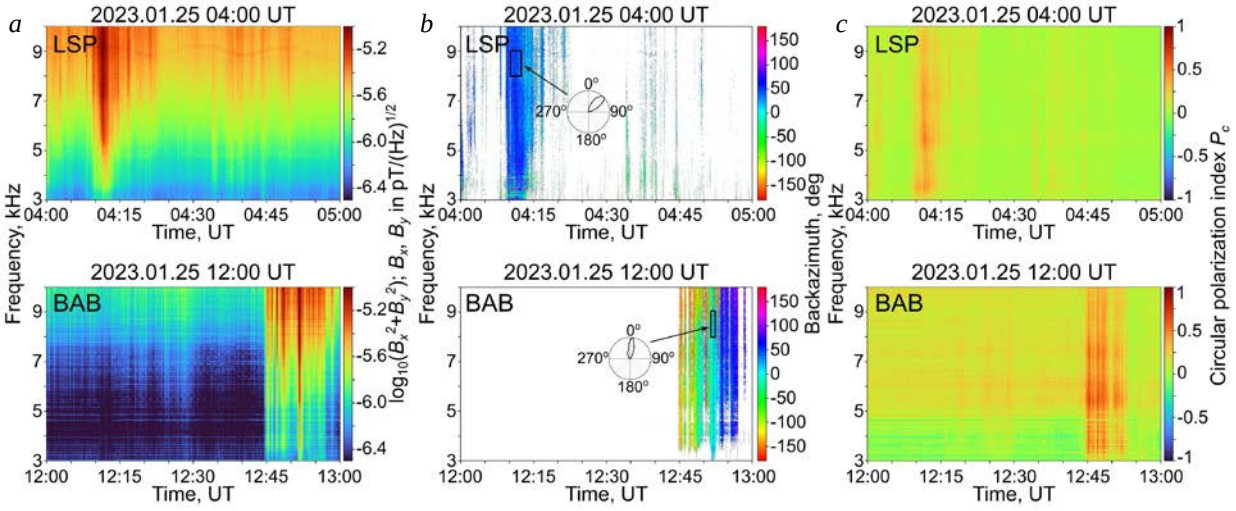

Figure 4. Frequency and time dependences of the power spectral density B_t (*a*), time-averaged φ_{bp} (*b*) and P_c (*c*) on LSP and at the Barentsburg Observatory (from top to bottom) for 04:00–05:00 UT and 12:00–13:00 UT on January 25, 2023, respectively. Additionally, the central panel illustrates normalized distributions of the energy flux density by φ_{bp} in polar coordinates for the selected sections of the spectrograms

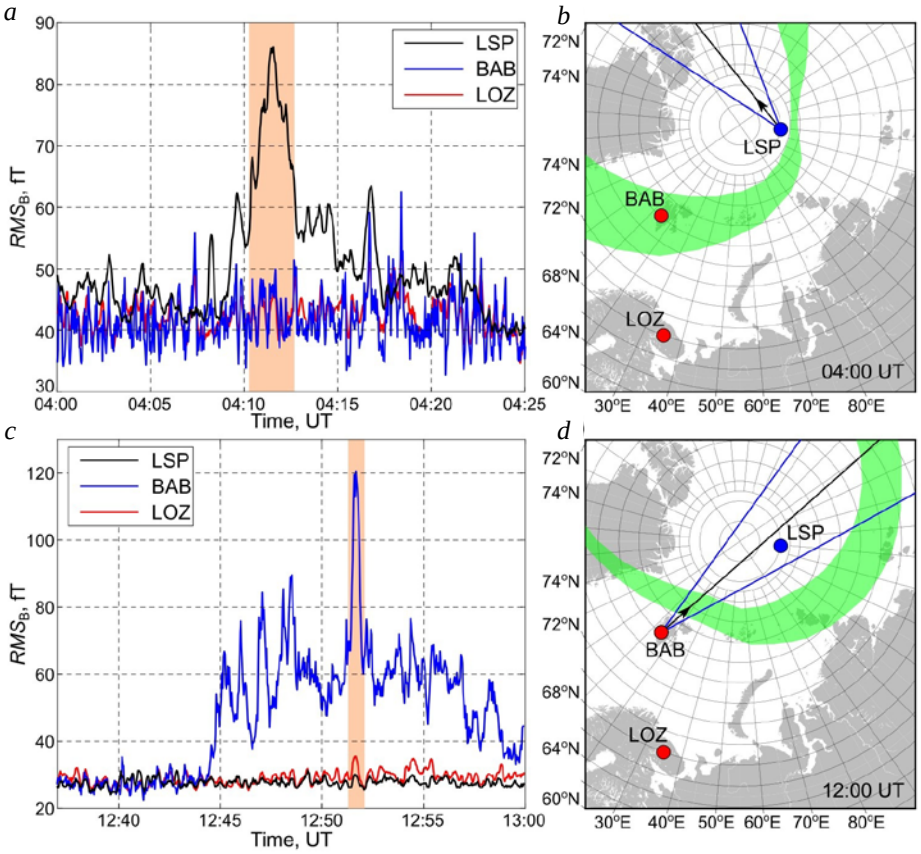

Figure 5. Time dependences of RMS_B in the 8–9 kHz frequency band for three stations: LSP (black curve), BAB (blue curve), and LOZ (red curve) for January 25, 2023 at 04:00 UT and 12:00 UT respectively (*a*, *c*); maps indicating the most likely direction to the hiss exit region (black line with arrow) and the range of possible directions (the area bounded by blue lines) for 04:00 UT and 12:00 UT respectively (*b*, *d*). The green color highlights the auroral oval

The March 12, 2024 event

In conclusion, let us consider the isolated short auroral hiss burst recorded on March 12, 2024 at 16:25 UT simultaneously at the three stations. At that time, the platform was near the Spitsbergen archipelago at a point with coordinates 83.3° N, 20.4° E. The distance between the platform and LOZ was 1740 km; and the distance between the platform and BAB, only 590 km. Geomagnetic conditions were quiet: $AL = -10$ nT, $Dst = -12$ nT.

The power spectral density B_t spectrograms (Figure 6, *a*) show that at 16:25 UT an isolated auroral hiss burst was recorded at all three stations. Analysis of the signal-to-noise ratio for this case has revealed that there were many atmospherics at 8–9 kHz frequencies that we failed to suppress during preprocessing. For further analysis, we, therefore, chose the 6–7 kHz band, where the signal-to-noise ratio is maximum. The envelopes B_t in the 6–7 kHz frequency band (Figure 7, *a*) indicate that this auroral hiss burst is on average 2–3 times smaller in amplitude than in the first two cases considered (January 24 and 25, 2023), and the amplitude at BAB here is almost 2 times larger than on LSP and at LOZ. Spectrograms of the polarization index P_c for this case are presented in Figure 6, *c*. During the observed hiss burst, polarization takes on the following values: $P_{c_{LSP}} = -0.33$, $P_{c_{BAB}} = -0.11$, $P_{c_{LOZ}} = -0.17$. The weak left-hand polarization, along with small RMS amplitudes of the hiss magnetic field horizontal component, indicates that the exit region is remote from each of the stations.

Distributions of time-averaged φ_{bp} (see Figure 6, *b*) of this event on LSP and at BAB are almost identical, and the similar distribution at LOZ differs greatly from them — it contains three lobes only one of which seems to correspond to the direction to the expected auroral hiss exit region (see Figure 7, *b*). It is directed northeast toward the auroral oval, is highlighted in blue in the φ_{bp} spectrogram, and is not found in any other segment of the spectrogram. We have analyzed the φ_{bp} distribution for noise for small time intervals before and after the hiss burst. It appeared that the noise consists mainly of atmospherics, the distribution of directions of which is oriented to the south-southwest. This direction corresponds to the African thunderstorm center, which should be active at this time (15–19 UT). The distribution also shows the south-southeast direction, highlighted in pink in the spectrogram and repeated in low-frequency noise (below 5 kHz) between 16:50 and 17:00 UT.

The March 12, 2024 event, as well as the previously discussed January 24, 2023 event, is characterized by the absence of geomagnetic disturbances. The coincidence of the envelopes of the RMS amplitudes is better than in the January 24, 2023 event, and close to ideal. The distance between LSP and LOZ was 1740 km, which is less than during the January 24, 2023 event, but

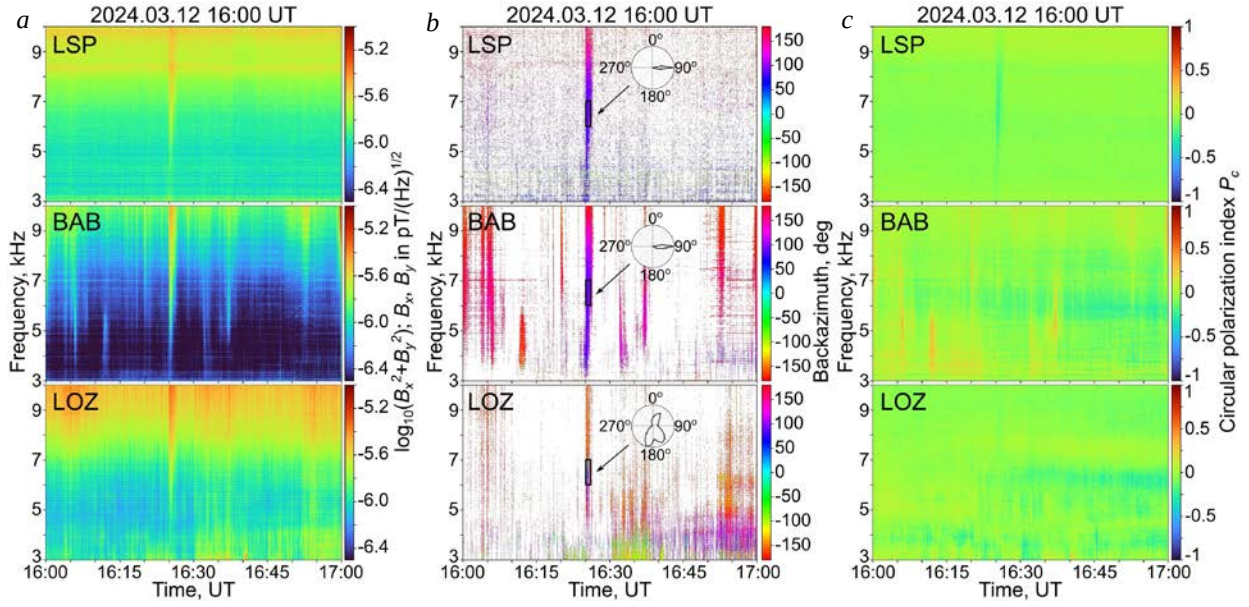

Figure 6. Time and frequency dependences of the power spectral density B_t (*a*), time-averaged φ_{bp} (*b*) and P_c (*c*) on LSP, at BAB, and LOZ (from top to bottom) for 16:00–17:00 UT on March 12, 2024. Additionally, the central panel illustrates normalized distributions of the energy flux density by φ_{bp} in polar coordinates for the selected sections of the spectrograms

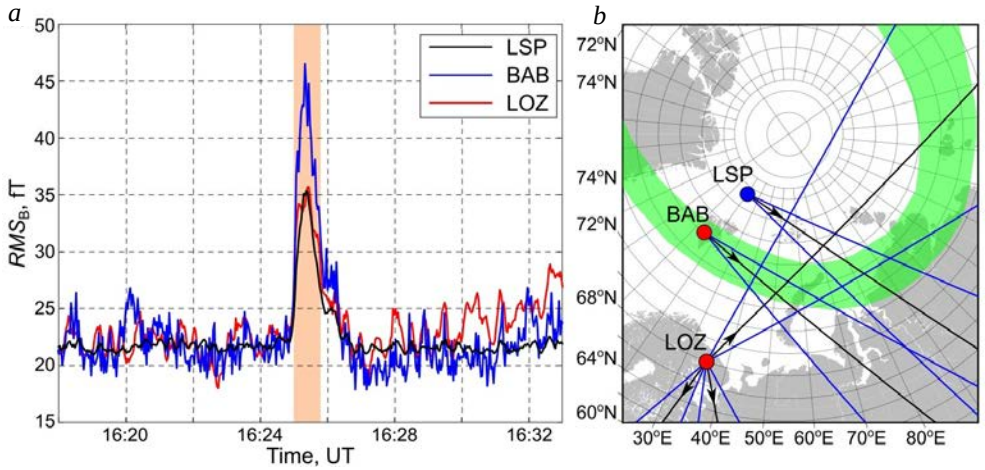

Figure 7. Time dependences of RMS_B in the 6–7 kHz frequency band for three stations: LSP (black curve), BAB (blue curve), and LOZ (red curve) for March 12, 2024 (*a*); a map indicating the most probable direction to the hiss exit region (black line with arrow) and the range of possible directions (area bounded by blue lines) (*b*). The green color highlights the auroral oval

large enough to consider the assumption of waveguide propagation of bursts improbable. Therefore, in our opinion, it is more likely that the auroral hiss bursts under study, as well as the bursts of the January 24, 2023 event, are caused by a spatially homogeneous flux of soft precipitating electrons, which triggered the generation of quasi-electrostatic waves, along with the presence of small-scale ionospheric irregularities in the vicinity of each of the three stations.

CONCLUSION

In 2022–2024, during the expedition at the North Pole–41 drifting polar station, the magnetic field horizontal components and the electric field vertical component were measured in the VLF range. Simultaneously with VLF observations at NP-41, the electromagnetic field components were measured at the Lovozero and Barentsburg observatories. The paper has briefly described the equipment, methods of data preprocessing, and the power spectral density, polarization, and energy flux directions of auroral hiss bursts obtained by these methods for each station.

We have analyzed three characteristic VLF events, in one of which (January 25, 2023) the locality of the auroral hiss region is manifested, and in the other two (January 24, 2023 and March 12, 2024) hiss bursts with envelopes of RMS amplitudes were simultaneously observed, which practically coincide at three points spaced up to 2600 km and 1740 km apart respectively. The locality of auroral hiss bursts has been repeatedly noted before, in particular in the circumpolar region during the Transarctic-2019 expedition. It is fair to assume that the locality is due to the small size of regions of small-scale

irregularities at 800–1200 km altitudes at which quasi-electrostatic waves are scattered thereby providing hiss propagation to the Earth surface.

The auroral hiss bursts recorded at the same time at the stations spaced several thousand kilometers apart with amplitudes that are well correlated with time (the January 24, 2023 event) or practically coincide (the March 12, 2024 event) have probably been observed for the first time. The assumption of propagation of VLF-hiss bursts from a single local exit region along the Earth—ionosphere waveguide to recording points, which explains the similarity between the bursts at large distances, is not confirmed either by the results of observations or by the results of modeling of the excitation of the Earth—ionosphere waveguide by a wave packet resulting from scattering of quasi-electrostatic waves by ionospheric irregularities. In our opinion, it is more likely to suspect a homogeneous flux of soft auroral electrons throughout the precipitation region, which generate quasi-electrostatic waves at altitudes 10–20 thousand km, along with the simultaneous presence of small-scale ionospheric irregularities in the vicinity of each of the three stations, where these waves are scattered into the propagation cone to the Earth surface.

The collected data is important for understanding the processes of generation and propagation of VLF waves in circumpolar regions and in the polar cap.

The observational data used in the paper was obtained during the expedition “Drifting Research Station “North Pole-41”, organized by the Arctic and Antarctic Research Institute (AARI) of Roshydromet on the basis of LSP North Pole. The expedition was funded within the framework of the Government assignment from AARI. We express profound gratitude to the members of the expedition, the crew of LSP North Pole, and the teams of the Lovozero and Barentsburg observatories for their comprehensive assistance in conducting the research.

REFERENCES

Budden K.G. The Propagation of Radio Waves: The Theory of Radio Waves of Low Power in the Ionosphere and Magnetosphere. *Cambridge University Press*, 1985, 669 p.

Gurnett D.A. A satellite study of VLF hiss. *J. Geophys. Res*. 1966, vol. 71, p. 5500.

Harang L., Larsen R. Radio wave emission in the VLF-band observed near the auroral zone. 1. Occurrence of the emissions during disturbances. *J. Atmos. Terr. Phys.* 1965, vol. 27 (4), pp. 481–497. DOI: 10.1016/0021-9169(65)90013-9.

Jørgensen T.S., Ungstrup E. Direct observation of correlation between auroras and hiss in Greenland. *Nature*. 1962, vol. 194, pp. 462–463. DOI: 10.1038/194462a0.

Kimura I. Effects of Ions on Whistler-Mode Ray Tracing. *Radio Sci*. 1966, vol. 1, no. 3, pp. 269–284. DOI: 10.1002/rds196613269.

Kleimenova N., Manninen Yu., Gromova L., et al. Bursts of auroral-hiss VLF emissions on the Earth’s surface at L~5.5 and geomagnetic disturbances. *Geomagnetism and Aeronomy*. 2019, vol. 59, iss. 3, pp. 272–280. DOI: 10.1134/S0016793219030083.

Lebed’ O.M., Fedorenko Y.V., Nikitenko A.S., et al. Modeling of the auroral hiss propagation from the source region to the ground. *Geomagnetism and Aeronomy*. 2019, vol. 59, no. 5, pp. 577–586. DOI: 10.1134/S0016793219050074.

Makita K. VLF/LF hiss emissions associated with aurora. *Memoirs of National Institute of Polar Research*. Tokyo. Ser. A, 1979, no. 16, pp. 1–126.

Manninen J., Kleimenova N., Kozyreva O., et al. Non-typical ground-based quasi-periodic VLF emissions observed at L 5.3 under quiet geomagnetic conditions at night. *J. Atmos. Solar-Terr. Phys*. 2013, vol. 99, pp. 123–128. DOI: 10.1016/j.jastp.2012.05.007.

Manninen J., Kleimenova N., Kozlovsky A., et al. Ground-based auroral hiss recorded in Northern Finland with reference to magnetic substorms. *Geophys. Res. Lett.* 2020, vol. 47. DOI: 10.1029/2019GL086285.

Means J.D. Use of the three-dimensional covariance matrix in analyzing the polarization properties of plane waves. *J. Geophys. Res.* (1896–1977). 1972, vol. 77, no. 28, pp. 5551–5559. DOI: 10.1029/JA077i028p05551.

Nikitenko A.S., Lebed O.M., Fedorenko Yu.V., et al. Estimating the size and location of the region of scattering of the auroral hiss, according to data from high-latitude observations at three separated places. *Bull. Russian Academy of Sciences: Physics*. 2021, vol. 85, no. 3, pp. 287–291. DOI: 10.3103/S1062873821030187.

Nikitenko A.S., Fedorenko Yu.V., Manninen J., et al. Modeling the spatial structure of the auroral hiss and comparing results to observations. *Bulletin of the Russian Academy of Sciences: Physics*. 2023, vol. 87 (1), pp. 112–117. DOI: 10.3103/S1062873822700265.

Pil’gaev S.V., Fedorenko Yu.V., Kleimenova N.G., et al. First results from VLF observations during the Transarctica–2019 polar expedition. *Geomagnetism and Aeronomy*, 2020, vol. 60, no. 2, pp. 212–215. DOI: 10.1134/S0016793220020127.

Pil’gaev S.V., Larchenko A.V., Fedorenko Y.V., et al. A three-component very low frequency signal receiver with precision data synchronization with universal time. *Pribory i tekhnika eksperimenta* [Instruments and Experimental Techniques]. 2021, no. 5, pp. 115–125. (In Russian). DOI: 10.31857/S0032816221040248.

Pilgaev S.V., Larchenko A.V., Filatov M.V., et al. A function generator for calibration of electromagnetic field recorders. *Pribory i tekhnika eksperimenta* [Instruments and Experimental Techniques]. 2018, no. 6, pp. 49–55. (In Russian). DOI: 10.1134/S0032816218060125.

Rytov S.M. *Vvedenie v statisticheskuyu radiofiziku* [Introduction to Statistical Radiophysics]. Moscow: Nauka Publ., 1966, 404 p. (In Russian).

Sazhin S.S., Bullough K., Hayakawa M. Auroral hiss: a review. *Planetary and Space Sci*. 1993, vol. 41, pp. 153–166. DOI: 10.1016/0032-0633(93)90045-4.

Sonwalkar V.S., Harikumar J. An explanation of ground observations of auroral hiss: Role of density depletions and meter-scale irregularities. *J. Geophys. Res.: Space Phys*. 2000, vol. 105, A8, pp. 18867–18883. DOI: 10.1029/1999JA000302.

Stix T. Waves in Plasmas. American Inst. of Physics, 1992.

Vorobjev V.G., Yagodkina O.I. Auroral precipitation dynamics during strong magnetic storms. *Geomagnetism and Aeronomy*. 2007, vol. 47, no. 2, pp. 185–192. DOI: 10.1134/s0016793207020065.

Yearby K.H., Smith A.J. The polarization of whistlers received on the ground near L=4. *J. Atmos. Terr. Phys*. 1994, vol. 56, no. 11, pp. 1499–1512. DOI: 10.1016/0021-9169(94)90117-1.

URL: http://apm.pgia.ru/ (accessed April 20, 2025).

Original Russian version: Lebed O.M., Pilgaev S.V., Larchenko A.V., Blagoveshchenskaya N.F., Kalishin A.S., Borisova T.D., Stribny O.Yu., Filatov M.V., Kuznetsova M.V., Nikitenko A.S., Beketova E.B., Fedorenko Yu.V., published in Solnechno-zemnaya fizika. 2026, vol. 12, no. 1, pp. 95–106. DOI: 10.12737/szf-121202610. © 2026 INFRA-M Academic Publishing House (Nauchno-Izdatelskii Tsentr INFRA-M).

How to cite this article

Lebed O.M., Pilgaev S.V., Larchenko A.V., Blagoveshchenskaya N.F., Kalishin A.S., Borisova T.D., Stribny O.Yu., Filatov M.V., Kuznetsova M.V., Nikitenko A.S., Beketova E.B., Fedorenko Yu.V. The first results of observations of auroral hiss during the «North Pole–41» expedition. *Sol.-Terr. Phys*. 2026, vol. 12, iss. 1, pp. 87–97. DOI: 10.12737/stp-121202610.